Computer Simulation of Molecular Exchange in Colloidal Systems

Alex Evilevitch,*,† Jurij Rescic,‡ Bengt Jönsson,§ and Ulf Olsson†

Division of Physical Chemistry 1 and Division of Biophysical Chemistry, Center for Chemistry and Chemical Engineering, Lund University, P.O. Box 124, SE-22100 Lund, Sweden, and Faculty of Chemistry and Chemical Technology, University of Ljubljana, P.O.Box 537, SI-1001 Ljubljana, Slovenia

Received: February 20, 2002; In Final Form: August 3, 2002

In this paper, we introduce two computer simulation models to study molecular exchange between aggregates in a colloidal dispersion. The Brownian motion of the colloidal aggregates is simulated as a random walk with a Gaussian distributed step length. In model I, the exchanging molecules are simulated as discrete particles with the exchange process characterized by desorption, molecular diffusion, and adsorption. A molecule desorbed from an aggregate is registered in the simulation and allowed to undergo individual Brownian motion until it adsorbs onto another colloidal aggregate or returns to the same aggregate from which it originated. In this detailed simulation, random size fluctuations are obtained in addition to a net variation in a relaxing, nonequilibrium size distribution. For many processes, net variations are very slow compared to the random fluctuations, making this detailed method very time consuming for studying a relaxing size distribution. For this reason, we also consider, in model II, a more approximate method where only the net flow of molecules between aggregates is considered. Here, the flow of molecules is for each time step calculated assuming steady state conditions and pair wise additivity. The flow between an isolated pair of aggregates can be solved exactly. Although the pair flow is a good approximation at short separations, it becomes significantly reduced at larger separations because of the presence of other aggregates. This screening of the flow at larger separations is accounted for by introducing an exponential damping function. With these models, we have simulated the solubilization of larger oil drops by smaller micelles which has previously been experimentally studied in a nonionic surfactant−water-oil system. Besides comparing with experiments, the simulations provides a test of a previous mean-field cell model analysis of the solubilization process.

1. Introduction

Many areas of current interest in technology and basic science involve the fundamental process of molecular exchange in colloidal systems.[1−3] This implies, molecular exchange in equilibrium systems and the process of relaxation in nonequilibrium systems with a net flow between the particles. This broad class of multiparticle diffusion problems includes, for example, coarsening phenomena, such as Ostwald ripening, nucleation and growth, and solubilization phenomena. The driving force for these processes might differ (in the system studied here, the driving force is the minimization of the curvature free energy of surfactant covered oil drops in water[4,5]); however, a complete theoretical description of the interparticle transport involves the solution of multi-coupled diffusion equations for the entire system. Such solutions are generally very difficult or impossible to obtain, and it is necessary to introduce simplifying approximations.

Several investigators have described colloidal systems undergoing molecular exchange with the help of different numerical simulation techniques.[6−15] Most of the models are developed to describe the coarsening process of Ostwald ripening. In the limit of low particle concentration, this process was originally discussed in the classic work of Lifshitz, Slyozov, and Wagner.[16,17] Much of the recent work in this area has focused on the corrections of the scaled size distribution function due to finite concentrations. We present here a new approach where two computer simulation techniques are used to describe the molecular exchange in a colloidal system. In the proposed simulation models, colloidal particles (in our case oil droplets) are moving in a Brownian motion at the same time as small molecules are allowed to exchange between the particles. As a case study, the two simulation models are applied to describe the molecular exchange of oil between microemulsion oil droplets in water. The solubilization of big oil drops by smaller microemulsion droplets transforms a bimodal size distribution into an equilibrium microemulsion with a unimodal size distribution. This process has been studied experimentally, and papers dealing with both the equilibrium properties,[18−21] as well as the nonequilibrium behavior,[22−25] have been published.

In a recent paper,[22] the solubilization kinetics was analyzed within the framework of a cell model. A good agreement with experiment could be found, and the cell model calculations could also account for the effects of droplet concentration on the solubilization rate. The object of the present computer simulation study is partly to test the cell model calculations. However, the simulations allow also for a more detailed study of the solubilization process, because the evolution of individual droplets can be followed in time. Furthermore, the computer simulations have the potential for analyzing effects of interpar-

* To whom correspondence should be addressed. Present address: University of California Los Angeles, Department of Chemistry and Biochemistry, 607 Charles E. Young Drive East, Box 951569, Los Angeles, CA 90095-1569. E-mail: evilevit@chem.ucla.edu.

† Division of Physical Chemistry 1, Lund University.

‡ University of Ljubljana.

§ Division of Biophysical Chemistry, Center for Chemistry and Chemical Engineering, Lund University.

10.1021/jp020467r CCC: $22.00
Published on Web 10/19/2002

ticle interactions on exchange kinetics, something that is not possible within the mean-field cell model approach.

The remaining part of the paper is divided into four parts. In section 2, we describe the simulation models and describe in detail how the Brownian motion of the particles is simulated and how the molecular exchange is modeled. In section 3, the experimental system that we aim to simulate is presented. Section 4 deals with the application of the simulation models to the process of oil resolubilization in microemulsion droplets. Finally, in section 5, we give some concluding remarks on the simulation model and its future use.

2. The Simulation Models

2.1. Brownian Motion of the Particles. In the simulation, the system is divided into equally sized cubical boxes, where all boxes and the content within them are equal at start and during the simulation. If a colloidal particle leaves a box at one box boundary, it automatically enters the same box at the opposite boundary (periodic boundary conditions). At the start of a simulation, the number and sizes of the colloidal particles in a box is specified and the particles are randomly placed in the box. As a case study, we are applying the simulation model to look at the process of oil resolubilization in the experimental model system of $C_{12}E_5$−decane−water microemulsion droplets.[22,23] In this case, the simulation starts with a discrete bimodal size distribution of droplets. Each box containing N_{big} big oil drops of radius R_{big} and N_{small} small oil droplets of radius R_{small}.

Droplet Overlap Test. If there is a particle overlap, the original configuration is rejected and a new one is generated. This test is also performed after each simulation loop, that is, when all of the droplets in the box have been moved. If two or more droplets overlap, the configuration is rejected, and all of the droplets are moved again to new positions.

For the simulated microemulsion droplet system of $C_{12}E_5$−decane−water, the droplets are modeled as hard spheres,[21] with a hard sphere radius, $R_{HS} = R_{hc} + \Delta R_{HS}$, where $\Delta R_{HS} = 10$ Å, as it was previously shown in ref 21. R_{hc} denotes the hydrocarbon radius of the droplet. This means that the minimum center-to-center inter-droplet separation is $R_{hc}^{droplet1} + R_{hc}^{droplet2} + 2\Delta R_{HS}$.

Interparticle Forces. At the same time as the center to center distances between the different particles in a box are calculated in the overlap test, the force on a particle, from interparticle interactions, can be obtained. However, in the simulations presented in this work, the interparticle forces are omitted, because these forces are rather weak in the $C_{12}E_5$−decane−water system. The effect of interparticle interactions on the interparticle molecular exchange will be more discussed in a coming paper.

Translation of a Particle in a Time Step, Δt. The change of the system, as a function of time, is in the simulation studied in repeated small time steps. In each time step, all particles in a box are translated in a Brownian motion, and the interparticle exchange of molecules is calculated. The length of a time step, Δt, is specified at the start of the simulation and is constant during the simulation. If the size of the particles is small the time step in a simulation needs to be rather short. This to restrict the translation of a particle to a distance comparable to the size of the particles in the studied system. As an example, if we use $\Delta t = 1 \times 10^{-9}$ s as the time step in a simulation of a $C_{12}E_5$−decane−water microemulsion system, the mean displacement, in this time step, of an oil droplet (with 61 Å radius) is 2.8 Å at 25 °C.

If interparticle forces between the colloidal particles can be neglected, the probability to find a particle that initially is located at (0, 0, 0) to be located in a volume element (dx, dy, dz) centered at (x, y, z) after a time step Δt is

$$p(x,y,z) = \frac{1}{\sigma^3}\varphi\left(\frac{x}{\sigma}\right)\varphi\left(\frac{y}{\sigma}\right)\varphi\left(\frac{z}{\sigma}\right) \mathrm{d}x\, \mathrm{d}y\, \mathrm{d}z \quad (1)$$

where

$$\sigma = \sqrt{2D^{\mathrm{p}}\Delta t} \quad (2)$$

D^{p} is the diffusion coefficient of the particle and $\varphi(x)$ is the Gaussian probability function. For spherical particles, the Stokes−Einstein relation can be used to determine the diffusion coefficient as a function of the radius of the particle. The equation for the parameter σ_i of particle "i" may then be written as

$$\sigma_i = \sqrt{2D_i^{\mathrm{p}}\Delta t} = \sqrt{2\frac{kT}{6\pi\eta R_i}\Delta t} \quad (3)$$

where k is the Boltzmann constant, T is the absolute temperature, η is the viscosity of the solution, and R_i is the radius of the particle.

The random steps in the x, y, and z directions that fulfill the probability distribution in eq 1 can be obtained by using Gaussian random numbers, see appendix A. With Gaussian random numbers, the steps in the x, y, and z directions become

$$\Delta x = \sigma\mathrm{GAUSS}_x, \quad \Delta y = \sigma\mathrm{GAUSS}_y, \quad \Delta z = \sigma\mathrm{GAUSS}_z \quad (4)$$

If there are strong forces between the colloidal particles, there is also a displacement of the particles originating from these forces. In this case, the translation function becomes

$$p(x,y,z) = \frac{1}{\sigma^3}\varphi\left(\frac{x - x_{\mathrm{f}}}{\sigma}\right)\varphi\left(\frac{y - y_{\mathrm{f}}}{\sigma}\right)\varphi\left(\frac{z - z_{\mathrm{f}}}{\sigma}\right) \mathrm{d}x\, \mathrm{d}y\, \mathrm{d}z \quad (5a)$$

where

$$(x_{\mathrm{f}},y_{\mathrm{f}},z_{\mathrm{f}}) = \frac{D^{\mathrm{p}}\Delta t}{kT}(F_x,F_y,F_z) \quad (5b)$$

Here, F_i is the force in the i direction acting on the studied particle.

When all of the colloidal aggregates in a box have been moved once, the exchange of small molecules between the aggregates during the time step, Δt, can be calculated. Two different models for this process will here be presented.

2.2. Simulation Model I: Discrete Molecular Exchange. *Exchange in a Time Step, Δt.* A natural way to approach the problem of molecular exchange is to also treat the exchanging molecules as discrete particles that undergo Brownian motion during the time when they are present in the continuous solvent. In the simulation, the colloidal aggregates move to new positions during the time step Δt. To describe the molecular exchange, we also have to consider the following three processes during Δt. (i) There is a probability that molecules associated with the aggregates disintegrate from the aggregates and enter the surrounding solution. (ii) The small molecules that earlier have disintegrated from the colloidal aggregates diffuse in the solution surrounding the aggregates. (iii) There is a probability that a small molecule adsorb to and integrate with an aggregate.

The most accurate way to handle this exchange process is to simulate, for each aggregate, the probability, in the time step

Δt, that a molecule is transported from the interior of an aggregate to a position outside the aggregate. A molecule that is outside an aggregate is in the coming simulation steps treated as a new independent particle that is transported by Brownian motion until it overlaps with an aggregate. A molecule that overlaps integrates with the aggregate and disappears as an independent molecule in the simulation. This simulation technique will here be called simulation model I.

If local chemical equilibrium is assumed between the interior of an aggregate and the region just outside the surface of an aggregate, the outgoing flow of molecules from an aggregate in a time step Δt can be written as

$$\mathrm{FLOW}_{\mathrm{out}} = 4\pi RDC(R)\Delta t \tag{6}$$

Here, R is the radius of the aggregate and $C(R)$ is the radius dependent equilibrium surface concentration. D is the diffusion coefficient of the small molecule in the continuous solvent.

The outgoing flow of small molecules from an aggregate, $\mathrm{FLOW}_{\mathrm{out}}$, is not the same as the number of molecules, that in a time step Δt, are transported from the interior of an aggregate to a position outside the aggregate. This number, N_{out}, is much higher because most of the molecules that are transported out from an aggregate diffuse back into the same aggregate. The connection between N_{out} and $\mathrm{FLOW}_{\mathrm{out}}$ can, for an isolated aggregate, be calculated from Fick's first law if steady state conditions are assumed. If all molecules that leave an aggregate initially are placed at the same distance R_{out} from the center of the aggregate, the connection becomes

$$N_{\mathrm{out}} = \mathrm{FLOW}_{\mathrm{out}} \frac{R_{\mathrm{out}}}{R_{\mathrm{out}} - R} \tag{7}$$

The distance R_{out} is in the present simulation chosen to be $R + R_{\mathrm{oil}}$, where R_{oil} the radius of the molecule that leaves the aggregate. This model gives, as long as $R_{\mathrm{oil}} \ll R_{\mathrm{out}}$, a nearly constant surface concentration of the small molecules, $C(R_{\mathrm{out}})$, even if other aggregates are in the neighborhood.

For the simulation case, considered in this paper, with oil microemulsion droplets in water, the net flow of oil monomers between different droplets arises from the difference in the radius dependent oil monomer concentration at the surface of each droplet. The radius dependent equilibrium surface concentration of oil monomers is given by eq 8 (derivation of this expression for the surface oil concentration is given in ref 23), see also Figure 1:

$$C(R) = C(\infty) \exp\left\{ -\frac{4\kappa' v_{\mathrm{m}}}{kT} \frac{(1 - Rc_0)c_0}{R^2} \right\} \tag{8}$$

where c_0 is the so-called preferred curvature of the surfactant film, κ' is the spherical bending modulus of the droplet/solvent interface,[5] $C(\infty)$ is the bulk phase solubility of oil, v_{m} is the molar volume of an oil monomer, and R is the radius of the droplet.

The probability that more than one molecule disintegrates from an aggregate can in most cases be neglected if the time step Δt is short. If this is the case, the simulation routine that checks if a molecule leaves an aggregate and creates a free molecule at the surface of the aggregate can be written as follows: (i) Create a random number between 0 and 1. A molecule has been desorbed from the droplet if the random number is less than N_{out} for the tested droplet. (ii) If a molecule has been desorbed, a new radius of the droplet is calculated from

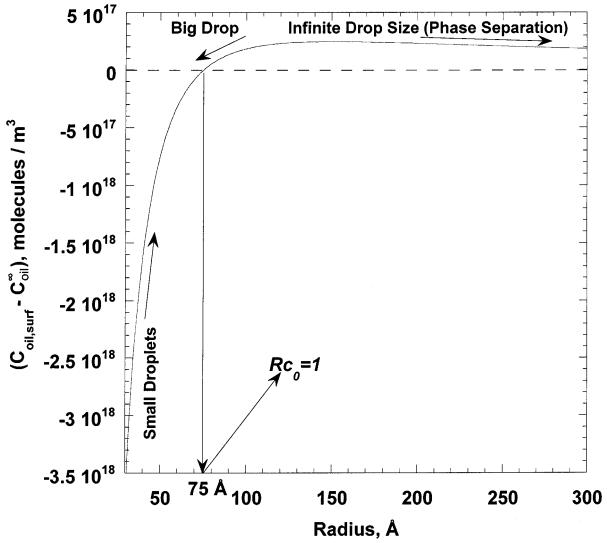

Figure 1. Difference between oil (decane) concentration at the surface of the droplet and the solubility of decane plotted as a function of drop(let)'s radius, for the system $C_{12}E_5$−decane−water at $\phi = 0.1$ (v/v).

$$R_{\mathrm{new}} = \left({R_{\mathrm{old}}}^3 - \frac{3V_0}{4\pi} \right)^{1/3} \tag{9}$$

where V_0 is the volume of the desorbed molecule. (iii) The random coordinates of the desorbed molecule, at the surface of the aggregate, can be obtained from eqs 10a−c, where the equations for RANSX, RANSY, and RANSZ can be found in appendix A:

$$x = x_{\mathrm{agg}} + R_{\mathrm{out}}\mathrm{RANSX} \tag{10a}$$

$$y = y_{\mathrm{agg}} + R_{\mathrm{out}}\mathrm{RANSY} \tag{10b}$$

$$z = z_{\mathrm{agg}} + R_{\mathrm{out}}\mathrm{RANSZ} \tag{10c}$$

(iv) The desorbed molecule is registered as a "free" particle that in the following time steps is displaced by a random Brownian motion.

In a simulation loop (simulating the processes that happens during the time step Δt), the processes i−iv are repeated for all colloidal aggregates before the Brownian motion of the desorbed molecules is calculated. The same type of procedure, as earlier discussed for the displacement of the colloidal aggregates, can also be used to calculate the displacement of the desorbed molecules. However, because the mobility of the free molecules is much higher than the mobility of the aggregates, the time step used in the simulation must be rather short to follow the motion of the desorbed molecules. To reduce the time for the simulation, we have chosen to use two different time steps in the simulation. The aggregates are moved once in the time step Δt, but the desorbed molecules are moved 10 times during the same time.

If a molecule, after a displacement, crosses the boundary of an aggregate, the molecule is integrated with the aggregate. The new volume of the aggregate then becomes

$$R_{\mathrm{new}} = \left({R_{\mathrm{old}}}^3 + \frac{3V_0}{4\pi} \right)^{1/3} \tag{11}$$

This completes one simulation loop. The total time of the molecular exchange process in a simulation is then given by, $t_{\mathrm{sim}} = N(\text{number of loops})\Delta t$.

For many systems, the net change of a relaxing size distribution is very slow compared to the random size fluctuations; hence, the net change corresponds only to a very small fraction of the molecular exchange events. However, the change from a nonequilibrium size distribution is always difficult to follow with this type of simulation because of the random size fluctuations. The simulation must either be repeated many times to reduce the noise or be followed for such a long time that the change toward equilibrium is much larger than the random fluctuations. This means that it is rather time-consuming to follow an equilibration process like solubilization with simulation method I, at least on a normal computer. Nevertheless, it captures individual exchange events and can be used to simulate processes such as the interdroplet exchange of fluorescent or phosphorescence probes and quenchers, often used to study microemulsion droplets,[26,27] or composition ripening in mixed particle systems.[28]

2.3. Simulation Model II: Net Flow of Molecules. *The Oil Flow between the Droplets.* To obtain a less time-consuming simulation procedure, suitable for slow relaxation processes, we now turn to a second model which only considers the net flow of molecules between the droplets rather than the individual exchange events. In this model, which we refer to as model II, the net flow is calculated for each time step by solving Fick's law. In doing so, we need, however, to make some simplifying assumptions concerning the concentration gradients.

To estimate the exchange of oil between the droplets in the box, we are doing the following approximations in simulation model II: (i) We assume the steady-state diffusion limit (we are not including any time dependence of the flow within the time, Δt). (ii) We set the concentration of oil monomers at the surface of each droplet as a radius-dependent function given by eq 8.[23] The function is plotted versus the droplet radius in Figure 1. (iii) We assume further that the total flow in the box is given by the sum of the pair flows between all pairs of droplets, where the flow between a pair of droplets is assumed being independent of the presence of other droplets. This assumption of additive pair flows is good enough for the total flow description at shorter separations between droplets (in comparison with the droplets' sizes), where the presence of other droplets does not affect the oil exchange. We would here also like to emphasize that the description of the oil flow between droplets at short separations is the most important part of the description of the total oil exchange process. The reason for this is that most of the oil exchange is indeed occurring at short interdroplet separations, as it was shown in our previous work[22] (see also the results below in section 4). However, at larger interdroplet separations, the pair-flow function will be significantly disturbed by other droplets, and the additive total flow of the pair flows will overestimate the real flow, see Figure 2. (iv) To correct for this deviation, we multiply the pair-flow function with a flow-damping factor. This damping factor was obtained in our previous work,[22] where a mean-field cell model was used to model the flow between oil droplets in a microemulsion. The effect of the damping factor is a reduction of the interaggregate flow at large separations as can be seen in Figure 2. The combination of the additive pair-flow method with the mean-field damping factor provides us with an approximate description of the oil flow in the box at all interdroplet separations.

The steady-state diffusive flow of oil molecules to and from a spherical droplet 1, with radius R_1 from another spherical droplet 2, with radius R_2, and a surrounding bulk solution is calculated in appendix B. In the calculations, it is assumed that

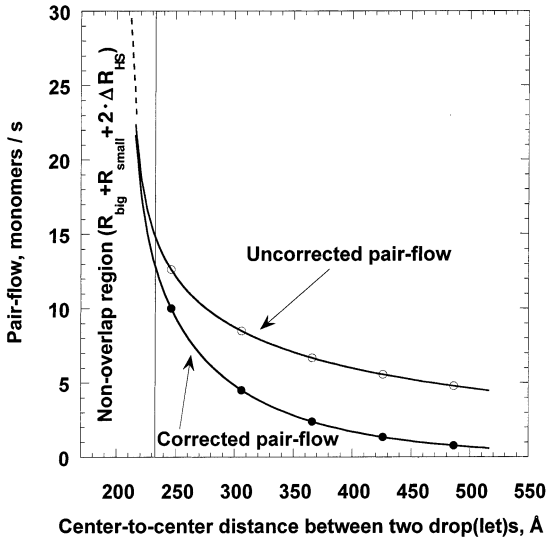

Figure 2. Molecular exchange function, describing the flow between two drop(let)s, plotted as a function of center-to-center distance between a droplet pair. (●) corrected pair-flow; (○) uncorrected pair-flow. The doted line is the extrapolation of pair-flow to infinity at the zero interdroplet separation.

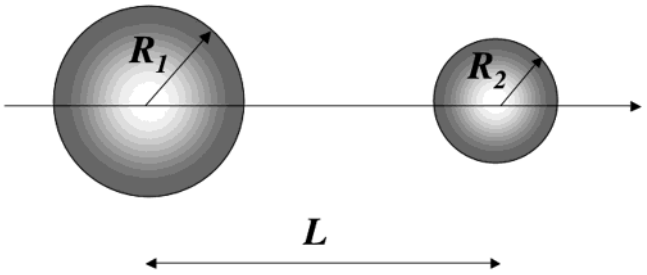

Figure 3. Steady-state diffusive flow of oil molecules calculated between two spherical droplets, droplet 1, with radius R_1 and droplet 2, with radius R_2, with center-to-center separation L.

the distance between the centers of the two droplets is $L_{1,2}$. The concentration of oil molecules in the water solution near the surface of each droplet is C_1 for droplet 1 and C_2 for droplet 2. The concentration of oil molecules in the bulk solution at an infinite distance from the two droplets is C_0, see Figure 3. The flow of oil into droplet 1 can be written as

$$Q_{1,2} = \Delta t D 4\pi R_1((C_0 - C_1) + (C_0 - C_1)G_{1,2} + (C_2 - C_0)F_{1,2}) \quad (12)$$

where the size and distance dependent parameters $F_{1,2}$ and $G_{1,2}$ in the range $0.1 < R_2/R_1 < 10$ approximately can be written as (see appendix B):

$$F_{1,2} \approx \frac{R_2}{L_{1,2}}\left(1 + 0.5 \ln\left(1 + \frac{1.770R_1R_2}{({L_{1,2}}^2 - (R_1 + R_2)^2)}\right)\right) \quad (13a)$$

and

$$G_{1,2} \approx 0.5\frac{R_2}{R_1 + R_2} \ln\left(1 + \frac{2R_1(R_1 + R_2)}{({L_{1,2}}^2 - (R_1 + R_2)^2)}\right) \quad (13b)$$

The first term in eq 12 represents the "undisturbed" flow of oil between droplet 1 and the surrounding bulk solution ("undisturbed" $= L_{1,2} \rightarrow \infty$). The second term represents the effect of droplet 2 on the flow of oil between droplet 1 and the surrounding bulk solution. The third term represents the flow of oil from droplet 2 into droplet 1.

In the simulation, we want to calculate the flow into droplet 1 from all of the droplets in the simulation box, as well as the flow from the surrounding bulk solution. If we, as an approximation, assume that the second and third terms in eq 12 can be added together for each droplet in the simulation box, the equation for the total flow of oil into droplet 1 can be written as

$$Q_1 = \Delta t D 4\pi R_1((C_0 - C_1) + (C_0 - C_1)\cdot\sum_{i=2}^{n} G_{1,i} + \sum_{i=2}^{n}(C_i - C_0)F_{1,i}) \quad (14)$$

Here, n is the total number of droplets in the simulation box and D is the diffusion coefficient of the oil monomers in water. Equation 14 describes the total oil flow between droplet 1 and all other droplets in the simulation box. However, because many particle effects are neglected in this equation, the flow from the droplets at large distances into droplet 1 is overestimated. This effect is mainly due to the screening of the "pair flow" by other droplets between the two droplets in the droplet pair. To correct for this overestimation, we multiply the flow exchange function between two droplets by an exponential damping factor derived in our previous description of the same droplet system with a mean-field cell model.[22] The exponential damping factor for the calculation of flow into droplet 1 from the rest of the droplets in the box is

$$E_{1,i} = \exp(-(\sum_{i=1}^{n}(\sqrt{C_i \cdot 4\pi R_i}))(L_{1,i} - R_1 - R_i)) \quad (15)$$

where C_i is the number density of droplet "i" in the box. The multiplication of the pair-flow exchange function between pairs of droplets (functions $F_{1,i}$ and $G_{1,i}$), given by eqs 13a,b, by the exponential function, $E_{1,i}$, suppresses the flow at larger interdroplet separations, whereas it does not affect the flow function at shorter separations, see Figure 2.

The final total flow exchange function that we use in the simulation thus becomes

$$Q_1 = \Delta t D 4\pi R_1((C_0 - C_1) + (C_0 - C_1)\sum_{i=2}^{n} G_{1,i}E_{1,i} + \sum_{i=2}^{n}(C_i - C_0)F_{1,i}E_{1,i}) \quad (16)$$

The only unknown parameter in eq 16 is the bulk oil concentration, C_0. However, this concentration can be calculated at the start of a simulation loop from the restriction that there is no external flow of oil to or from the simulation box. This restriction means that

$$4\pi D\sum_{i=1}^{n} R_i(C_0 - C_i) = 0 \quad (17)$$

or

$$C_0 = \frac{\sum_{i=1}^{n} R_i \cdot C_i}{\sum_{i=1}^{n} R_i} \quad (18)$$

This completes the presentation of all of the necessary equations and algorithms needed to set up the simulation routine, and we can now go on to give a short presentation of the experimental system used as an example of the potential of the proposed simulation technique. Here, we study the resolubilization of big oil drops by smaller microemulsion droplets in the $C_{12}E_5$−decane−water microemulsion system. A process that transforms a bimodal size distribution into an equilibrium microemulsion with an unimodal size distribution.

3. The Experimental Model System

As a case study for our simulation models, we are using here a well characterized nonionic surfactant−oil−water system ($C_{12}E_5$−decane−water) for which we have recently investigated the phase separation of excess oil from an oil-in-water droplet microemulsion.[5,24,25] The nonionic surfactants of the ethylene oxide type have a strongly temperature-dependent spontaneous curvature, and phase separation is conveniently generated by lowering the temperature. The process involves the disproportionation, by nucleation and growth, of a few droplets of the population that grows in size, allowing the majority of droplets to shrink. When the shrinking droplets have reached their new equilibrium size, the big drops continue to evolve by Ostwald ripening. In this work, we consider the reverse process where oil is solubilized by the microemulsion droplets. A droplet microemulsion sample is initially temperature quenched from the phase boundary into the two-phase area, where the droplets at equilibrium coexist with excess oil, and then left for some time to allow the nucleation and growth of larger droplets. Thus, the original unimodal size distribution is split into a bimodal size distribution of larger and smaller droplets compared to the original average size (we choose to term here the larger droplets as "drops" and the smaller ones as "droplets" throughout the paper). At a certain time after the quench, the temperature is reversed back to the initial temperature. As a result, the system reverts back into the original unimodal size distribution by having the large drops solubilized by the small droplets.

At a surfactant-to-oil volume fraction ratio of $\phi_s/\phi_o = 0.815$, a water-rich (oil-in-water) microemulsion phase is stable in the temperature range from 25 to 32 °C, whereas below 25 °C, the microemulsion phase separates with essentially pure oil as the second phase.[29] At the $L_1/(L_1+O)$ phase boundary at 25 °C, which is remarkably independent of water concentration, the solution consists of spherical microemulsion oil droplets corresponding to the maximum curvature toward oil given the constraint of the area-to-enclosed volume ratio imposed by the ratio ϕ_s/ϕ_o.[19] The hydrocarbon radius is approximately 75 Å, the polydispersity is low, and structural and dynamical properties follow closely those of a hard sphere fluid.[18,19] When the temperature is decreased below 25 °C, the preferred curvature toward oil increases, and when equilibrium is reached, the microemulsion droplets have decreased in size and excess oil has diffused from small droplets to the newly nucleated larger drops. From there on, the population of large drops continues to evolve through a classical Ostwald ripening process.[24] Because of the 2 orders of magnitude higher monomeric solubility of the surfactant compared to the oil, we can assume that the surfactant redistributes fast and that the rate-limiting step of the relaxation process is the redistribution of oil.

Resolubilization Experiment. Experiments have been performed on the $\phi = 0.1$ (v/v) $C_{12}E_5$ and decane microemulsion oil droplets in water. The sample was first equilibrated at 25 °C, for a couple of hours, and the turbidity was measured to ensure that its value was constant in time. Then, the sample was temperature-quenched in the two-phase region, by placing it in a 22 °C water bath and keeping it there for 2 h. After 2 h,

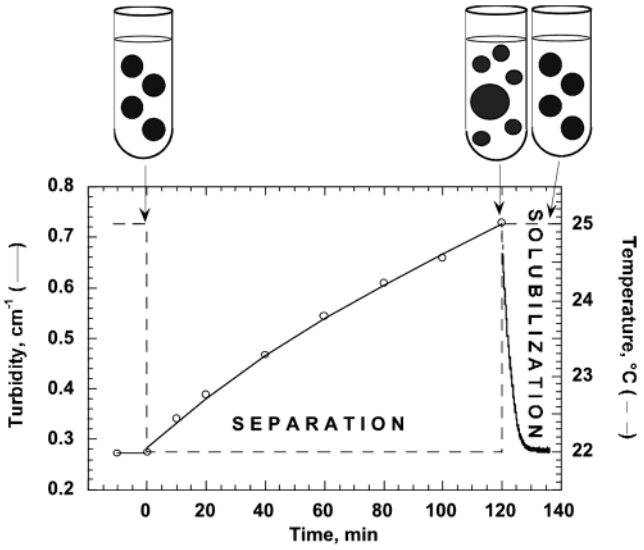

Figure 4. Variation of turbidity with time for the temperature jump from 22 to 25 °C after 120 min at 22 °C, with the volume fraction $\phi = 0.1$ (v/v) (●). The doted line is the extrapolation to the time of the temperature jump. The solid line is the relaxation rate obtained from the cell model calculations in ref 22.

the initially monodisperse microemulsion droplet system with $R_{hc} = 75$ Å has transformed into a droplet solution with two narrow size distributions. The phase separating oil was resolubilized by bringing the sample back to 25 °C. The entire sample was always immersed into the thermostated water of the required temperature. In this way, temperature gradients within the sample could be minimized. The turbidity of the sample was traced continually with time, at $\lambda = 406$ nm using a Perkin-Elmer Lambda 14 UV/visible spectrophotometer, containing a thermostated sample cell holder, see Figure 4.

4. Simulation Results

The initial resolubilization of big oil drops by small oil droplets was simulated by both simulation techniques presented above. As a starting point for the simulations, a system that consists of two distinct droplet populations with initial average radius classified in the input parameters as R_{big} and R_{small} is assumed. In the simulation, we are placing a two size population of randomly distributed big drops (with number N_{big}) and small droplets (with number N_{small}) in a simulation box. The total volume fraction of drop(let)s is $\phi = 0.1$, like in the experimental system (for simplicity and shorter computation times, in most of the simulation cases we chose to have only one big drop per box). The initial input parameters in the simulation are R_{big} (initial) = 150 Å, R_{small} (initial) = 61 Å, $D = 9.5 \times 10^{-10}$ m^2/s (for decane in water at 25 °C),[30] $C_{oil}^{\infty} = 2.16797 \times 10^{20}$ m^{-3} (for decane in water at 25 °C),[31] $v_o = 323 \times 10^{-30}$ m^3, $c_0 = 1/75 \times 10^{-10}$ m^{-1}, $\kappa' = 1.5kT$.[32]

In the simulation, we choose the mean displacement of a small droplet to be around 2.5 Å (and ≈1.5 Å for the big one). The choice of such a small displacement step will ensure that the droplets will occupy as many positions in the box as possible, imitating the Brownian motion in the real system. A small displacement step will also minimize the number of configurations where the droplets overlap. The choice of such displacement step, in accordance with the Stokes−Einstein relation, corresponds to a time step of 0.5×10^{-9} s (with this time step 99.4% of configurations are accepted).

4.1. Simulation Model I. *Analysis of the Initial Oil Flow from the Big Droplet.* The changes of the number of solubilized oil molecules in the big droplet during the first millisecond have been studied with simulation method I, where the transport of all exchanging molecules is followed. The results from four such simulations are presented in Figure 5 together with the average results from 10 simulations. From these simulations, it is clear that the fluctuation in size is much larger for the studied system than the average change during a millisecond. This is not a surprise because the difference in oil concentration, at the surface of the droplets, has a rather weak dependence on the droplet radius, as can be seen in eq 8. The small fluctuations seen in the average curve of the 10 simulations is a coincidence, more than a thousand simulations are needed to average out the fluctuations to a level where the average reduction of the number of oil molecules in a big droplet can be seen. Instead of making many simulations the length of a simulation can be increased. Both experiments and simulations shows that the time the system in the simulation needs to be studied, to obtain an average decrease in the number of oil molecules in a big droplet comparable with the size fluctuations, is 1−10 s. This means that for the present system we cannot follow the whole resolubilization process. We therefore turn to the second method where only the net flow of oil molecules is simulated.

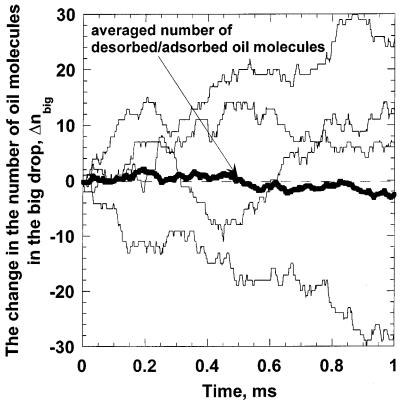

Figure 5. Simulated change in the number of oil molecules in a big micelle as a function of time.

4.2. Simulation Model II. *Analysis of the Equilibration of Nonequilibrium Droplets.* Considering the fact that the whole resolubilization process in the real system takes ≈15 min, the choice of a 10^{-9} s time step implies that each droplet is displaced ≈10^{12} times during the simulation. Because, the simulation of the whole process would take unrealistically long computing time and thus would only be possible for the droplet systems with much higher oil solubility, we have simulated oil resolubilization in this $C_{12}E_5$−decane−water system using the following procedure.

(i) The simulation starts with one big drop and N_{small} small droplets. Resolubilization is simulated during 1 ms, and the total flow from the big drop as well as individual oil flows between droplets are evaluated. The total mean displacement of a small droplet during this simulation time is then 2.5×10^6Å, which is much longer than the box dimensions (box side = 813 Å). This ensures that each droplet has moved many times across the whole box and a good prediction of the oil flow from the big drop can be obtained. Because the oil flow during this short simulation time is very low, only small changes in droplet size can be observed in this simulation. Individual droplet sizes are also recorded as a function of time during the simulation.

(ii) From the simulation in i, the initial oil flow and the derivative of flow from the big drop at time t_1 is obtained. The 1 ms simulation is now repeated for a new configuration of droplets at time t_2, where the big drop has shrunk in size while

the small droplets became larger. The new input parameters N_{small}, R_{small}, or R_{big} are chosen so that the total concentration of oil and the total interfacial area of the droplets in the box remains constant. The conservation of total area (A) and volume (V) implies

$$A = 4\pi N_{small} R_{small}^{\ 2} + 4\pi N_{big} R_{big}^{\ 2} \tag{19}$$

and

$$V = 4/3\pi N_{small} R_{small}^{\ 3} + 4/3\pi N_{big} R_{big}^{\ 3} \tag{20}$$

Thus, by fixing one of the parameters N_{small}, R_{small}, or R_{big} in eqs 19 and 20, where N_{small} is an integer, and setting $N_{big} = 1$ within one box, one obtains the other two parameters.

(iii) Simulations with duration 1 ms are repeated at different droplet sizes so that N_{small} remains an integer. R_{big} was varied between 79 and 150 Å, and correspondingly, R_{small} was varied between 61 and 74 Å. This resulted in nine simulation steps with different droplet sizes and numbers. In the first seven simulations, we had one big drop, and the number of small droplets was varying between 24 and 32 droplets per box. In the last two simulations, where the sizes of small and big drop(let)s were becoming similar, we had to increase the simulation box size by increasing the number of big drops together with small droplets, to keep N_{small} and N_{big} as integer parameters, while the area and the volume were kept the same as in the previous simulations. This was not necessarily in the cell model, where we only had one big drop and the number of small droplets was not an integer and could be changed continuously. So, for instance, in the last simulation data point, the parameters were $R_{small} = 74.8$ Å, $R_{big} = 79.6$ Å, $N_{small} = 171$, and $N_{big} = 7$. The oil flow from the big drop as a function of drop's size could now be obtained from these simulations.

(iv) From the connection between the flow and big drop's radius obtained in ii and the mass balance, the full time dependence of the oil transport from the big drop to the small droplets could be obtained using the Euler−Maclaurin summation formula:

$$\int_{t_1}^{t_2} Q(t)\,\mathrm{d}t = V(t_2) - V(t_1) \approx \left(\frac{\mathrm{d}Q(t_1) + \mathrm{d}Q(t_2)}{2}\right)(t_2 - t_1) - \frac{1}{12}\left(\frac{\mathrm{d}Q}{\mathrm{d}t}(t_2) - \frac{\mathrm{d}Q}{\mathrm{d}t}(t_1)\right)(t_2 - t_1)^2 \tag{21}$$

where $Q(t)$ is the total flow out from the big drop at time t and $V(t)$ is the volume of the big drop at time t.

The total flow out from the big drop as a function of time is presented in Figure 6. In this figure, the simulated flow is plotted together with the flow data obtained with the cell model approach. A good agreement in the flow data obtained with these two models illustrates that the previously made assumptions in our cell model are reasonable.

By setting all of the small droplets to be equally sized in the beginning of every new 1 ms simulation, we have been assuming that all small droplets are growing in size simultaneously and small size variations between them can be neglected. The validity of this assumption is discussed bellow.

Analysis of the Droplets Size Distribution. Because our simulation models allow us to keep track of the oil flow to and from discrete droplets, we can look at the size variation of every droplet as a function of time. However, because of the very short simulation times, radius increment of the small droplets will be very small. Therefore, for better visualization, we choose to look at the size change of small droplets compared to the initial size, calculated as the number of oil molecules in each droplet at the time t, minus the initial number of oil molecules in the droplet, at the time zero, $\Delta n = n - n(0)$. In Figure 7, Δn for each small droplet is plotted from a 0.5 ms long simulation at the times 0.25 and 0.5 ms. The figure shows that the deviation in Δn, for each small droplet, is small compared to the change in the mean Δn value. This illustrates that the assumption of monodisperse small droplets at the start of each 1 ms long simulation is not a too severe approximation.

The fact that all of the small droplets are simultaneously increasing in size, without a significant size gradient within the box, is mainly an effect of the low oil flow between the droplets compared with the rapid mixing of the droplets. Although the oil flow from a big oil droplet to its nearest neighbors is much higher than to droplets at greater distances, see Figure 2, the Brownian motion of the droplets equalize the mean interdroplet distance even at such a short time as 0.25 ms. Another equalizing

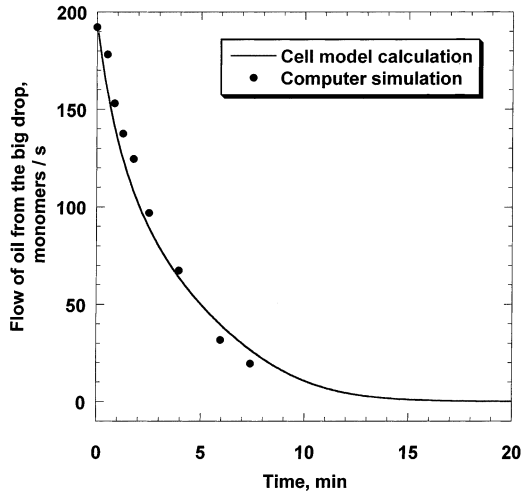

Figure 6. Total flow out from the big drop plotted as a function of time for the temperature jump experiment from 22 to 25 °C after 120 min at 22 °C. The simulated flow (●) is plotted together with the flow data obtained with the cell model approach in ref 22 (solid line).

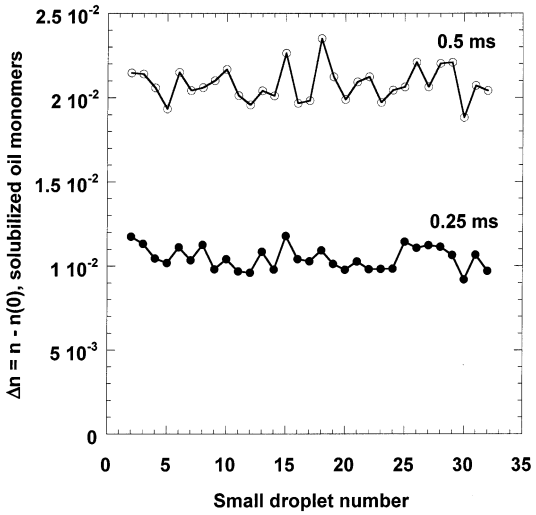

Figure 7. Number of oil molecules solubilized by each droplet, calculated as the number of oil molecules in each droplet at the time t, minus the initial number of oil molecules in the droplet, at the time zero, $\Delta n = n - n(0)$. Δn is shown for each small droplet plotted from the 0.5 ms long simulation at times 0.25 (●) and 0.5 ms (○). The solid lines, interconnecting the data points, are just guides for the eye.

factor is that the small droplets also exchange oil molecules with each other, so that the small droplets coming from the vicinity of a big drop equilibrates its oil content with the surrounding droplets when moving away from the big drop. Which of these two processes is the dominant mechanism for the interdroplet oil exchange will be analyzed below.

Analysis of Oil Exchange between Nonequilibrium Droplets. Above, we have proposed two main reasons why the small droplets in our microemulsion are growing simultaneously in size during the resolubilization process, and we will here give a more detailed discussion of this phenomena. The behavior can partly be explained by the diffusional mixing of the droplets. This effect becomes clear when the flow of oil monomers and the mobility of the oil droplets in the simulation box is considered. The time is takes for a small droplet to diffuse from the center to the boundary of a simulation box can be estimated by

$$\tau_d = \frac{(l/2)^2}{6D^{\text{droplet}}} \tag{22}$$

where l is the length of the box side. In our system, with $l = 813 \times 10^{-10}$ m and $D^{\text{droplet}} = 10^{-11}$ m^2/s, this diffusion time of a droplet is $\tau_d \approx 10^{-5}$. In the simulation experiment shown in Figure 7, we have been looking at the size distribution of the droplets on the time scale of 0.25×10^{-3} s. Even within such a short time, each droplet will cross the simulation box many times. That is, droplets exchange their positions very fast, so that on the time scale of the slow oil resolubilization process which takes minutes (because of the slow flow of oil monomers out from the big drop), all of the small droplets in the system will experience the same mean in-flow of oil coming from the big drop. In other words, for $t \gg \tau_d$, the system is in the mean-field limit.

Now, we return to the question of whether the exchange of oil molecules between the small droplets themselves significantly contributes to the simultaneous droplet growth. In the previously derived cell model for the same microemulsion droplet system, we have shown that all of the oil is solubilized in the small droplets mainly in the vicinity of the big drop. Further out from the surface of the big drop, at some critical distance $r = \delta$ (which we have previously termed "the solubilization layer"), there will be almost no oil monomers left to solubilize. The simulation gives the same picture. In Figure 8, we have plotted the probability function $P(r)$, of solubilizing oil monomers within the volume element dV at the distance r from the center of the big drop. The probability function $P(r)$ is thus calculated in a 1 ms long simulation as an average number of oil molecules solubilized per second in small droplets within a spherical shell of thickness Δr (concentric with the big drop, with one big drop in the box). To normalize the result, we have divided the number by the volume of the corresponding spherical shell and also by the total flow of oil out from the big drop. For simplicity, only one big drop is placed in the box, and this drop is fixed in the center of the box. Figure 8 nicely illustrates that the probability of finding oil molecules, which can be solubilized by the small droplets, is high closer to the big drop (within the solubilization layer), whereas it is almost zero further out from the big drop. Oil is thus solubilized in the small droplets mainly within the solubilization layer. This once again illustrates the above-mentioned statement that our pair-flow exchange function, which gives the correct flow expression only at shorter interdroplet separations (without the mean-field correction), gives a good description of the oil exchange process,

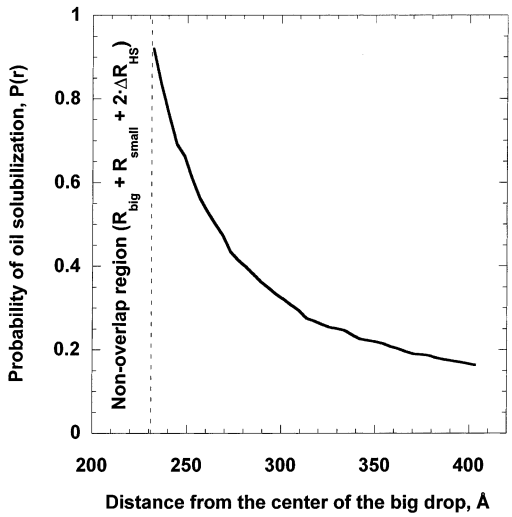

Figure 8. Probability function $P(r)$, for the temperature jump experiment from 22 to 25 °C after 120 min at 22 °C. The system is $C_{12}E_5$−decane−water at $\phi = 0.1$ (v/v). Function $P(r)$ shows the probability of finding free oil molecules in the bulk, which can be solubilized by the small droplets. $P(r)$ is high closer to the big drop, whereas it is almost zero further out from the big drop.

because it is occurring mainly at the short distances from the droplets. However, the time a small droplet spends in the vicinity of the big drop is rather short, as can be estimated by eq 23, where $\delta \approx 100$ Å:

$$\tau_\delta = \frac{\delta^2}{6D^{\text{droplet}}} \tag{23}$$

For our system, the lifetime τ_δ of a small droplet within the oil solubilization layer will be of the order of 10^{-6} s. The flow of oil monomers from the big drop into one small droplet is approximately ≈25 monomers/s (as it was calculated in the simulation). Thus, each small droplet will on average solubilize only 25×10^{-7} monomers during the time τ_δ, when the droplet is close to the big drop. Because of the small average amount of oil solubilized by the small droplets (during the very short time τ_δ) in the vicinity of the big drop, these droplets will not differ in size significantly from the small droplets, which are further out from the big drop. Because there is almost no difference in size between the small droplets, there will not be any significant surface concentration gradients of the oil among small droplets (since oil surface concentration is radius dependent). This results into negligible flows of oil monomers within the population of the small droplets.

This mechanism of oil exchange between the droplets can be illustrated by the simulation results shown in Figure 9 parts a and b. In Figure 9a, we have plotted the total flow of oil out from the big drop as a function of time. In Figure 9b, we have plotted the total flow of oil versus time into one small droplet selected in the simulation. Both flows are calculated in the same simulation and are shown in the figures during the first 70 μs of time. In the same figure, we have plotted the distance variation between this selected droplet and the big drop. From Figure 9a, we can observe that the flow from the big drop almost is time independent for such a short simulation time. This is due to the fact that on average there is the same number of small droplets solubilizing oil in the vicinity of the big drop. On the contrary, the in-flow of oil into a small droplet in Figure 9b is fluctuating in time, because of the changes in the distance to the big drop (up to 5 times difference in the flow during 70 μs simulation time, as shown in the figure). This illustrates that

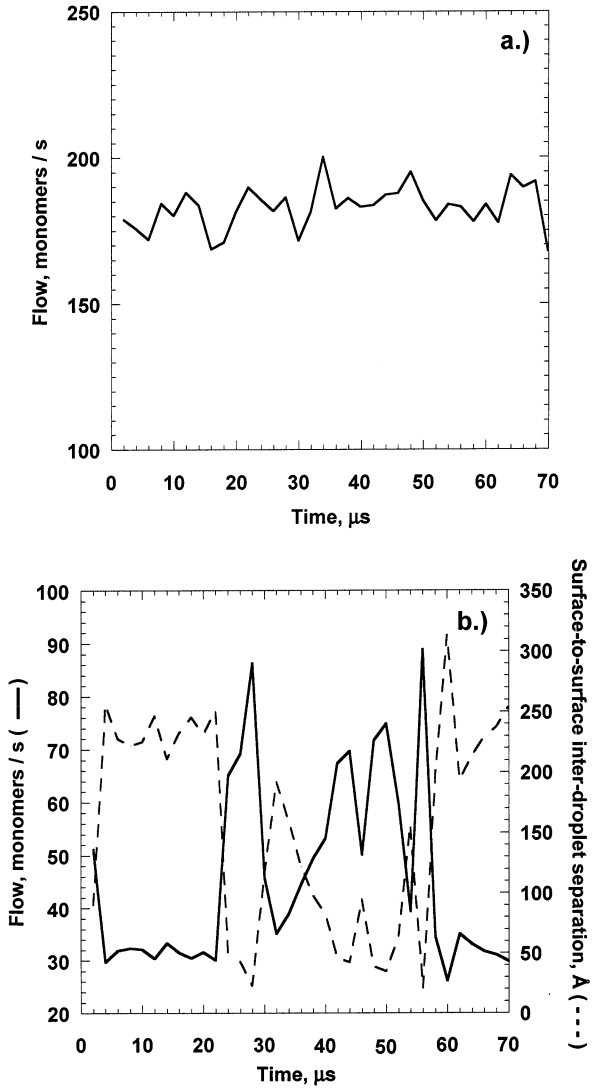

Figure 9. a. Total flow of oil out from the big drop plotted as a function of time. b. Total in-flow of oil into one small selected droplet plotted as a function of time during the simulation (solid line). In Figure 9b, we have also plotted the distance variation between this selected droplet and the big drop (dotted line). Both flows are calculated in the same simulation and are shown in the figures during the first 70 μs of time. The simulation describes the temperature jump experiment from 22 to 25 °C after 120 min at 22 °C.

the small droplets mainly change their oil content when they are in the vicinity of a big drop. Thus, the main oil flow is coming directly to the small droplets from the big drop and not from other small droplets.

Therefore, we conclude that the small droplets are growing in size simultaneously, where all of the oil is solubilized directly from the big drop and the mutual oil exchange between small droplets can be neglected. This result proves again the validity of another simplification made in the cell model, where we have just been treating the flow from the big drop directly to the small ones, whereas the exchange of oil between the small droplets was neglected.

Effect of Droplet Concentration on Oil Flows in the System. In our cell model approach,[22] we have been analyzing the effect of the small droplet concentration of the resolubilization kinetics. It is experimentally observed that an increase in droplet concentration increases the resolubilization rate. From the analytically derived cell model expression, it is clear that the faster resolubilization rates at higher droplet concentrations are due to the decrease of the solubilization layer thickness δ, see ref 22.

Our simulation gives the same picture, see Figure 10. In this figure, we have plotted the total flow from the big drop to the surrounding solution during 1 ms time for the systems with one big drop and with 14 and 29 small droplets, respectively. All of the other parameters for both systems were the same. From the figure, we see that the flow out from the big drop increases when the number of small droplets per big drop increase. Thus, the number density of "sinks" in the vicinity of the big drop clearly affects the solubilization rate. Setting the number of small droplets in the box to zero, gives the flow equal to the flow calculated with the analytical model for the infinite dilution limit (IDL approximation),[22,23] see Figure 10.

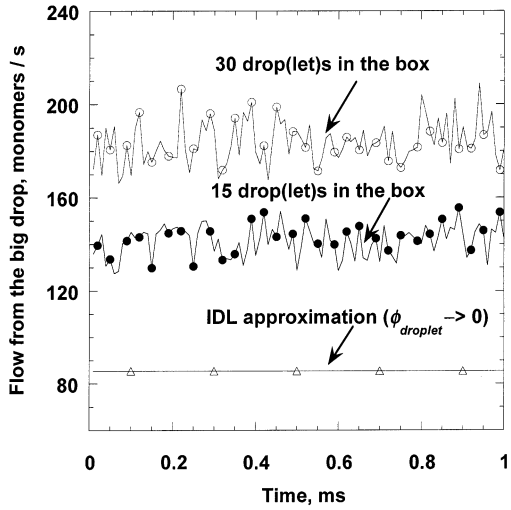

Figure 10. Total flow from the big drop to the bulk with small droplets plotted as a function of time, during 1 ms long simulation. The flow is plotted for the simulated systems with 30 drop(let)s (○), respectively, 15 drop(let)s (●) in the box. Simulated oil flow from the big drop at $\phi_{\text{droplet}} \rightarrow 0$ is also plotted in the Figure (Δ).

5. Concluding Remarks

In this paper, we have introduced two computer simulation models to study the molecular exchange between colloidal aggregates undergoing Brownian motion in solution. As an example, we have considered the exchange of oil molecules between microemulsion/emulsion oil droplets in water. In simulation method I, the exchanging molecules are individually traced in the simulation as particles also undergoing a Brownian motion. The molecules are released from the colloidal aggregates by a random process, simulating the finite lifetime of a molecule in an aggregate. A molecule in the solvent is absorbed when colliding with an aggregate thus following diffusion controlled kinetics. However, because of the small number of aggregates in the studied system the simulation must be repeated many times to average the random fluctuations. This makes this simulation process rather time consuming. An alternative way of modeling the exchange is to use continuum description of the net flow of molecules between the aggregates, simulation model II. However, this can only be done if the flow is approximated as the sum of pairwise additive flows. Because of multiparticle effects, this is a much more approximate method than to follow each exchanging molecule. To reduce the errors, from multiparticle effects in the continuum description an exponential damping factor is introduced.

Using the continuum approach, we have simulated the process where a low concentration of bigger oil drops are solubilized

by a larger concentration of smaller droplets, corresponding to the relaxation of a bimodal size distribution into a unimodal one. The object was to simulate solubilization in a nonionic surfactant−water−oil system[22] for which experimental data are available. Using input data from the experimental system, the simulation result was consistent with the experimentally observed solubilization rate. The simulation results were also consistent with a previous analytical mean field analysis using a cell model approach. The fact that the oil is absorbed by the small droplets predominantly near a big drop was confirmed by the simulation.

The simulation allows us to investigate details of the solubilization process as well as how the rate varies with parameters like droplet size and concentration. Furthermore, the proposed simulation technique allows us to investigate the influence, on the solubilization rate, of interparticle interactions. In the present simulation, aimed to simulate a nonionic system, the droplets interacted through excluded volume interactions only. However, the simulation can easily be extended to include other forms of pair interactions. Because of the distance dependence of the molecular flow, particle−particle interactions are expected to strongly influence the solubilization rates in many systems. Our intention is to use the proposed simulation technique, as a tool, to understand and interpret the dynamic processes observed in the different colloidal systems that we have studied.

Acknowledgment. This work was supported by The Swedish Foundation for Strategic Research (SSF program for Colloid and Interface Technology).

Appendix A

We have used the following procedure to obtain Gaussian random numbers: (i) Generate a random number between 0 and 1, here called RANX. (ii) Calculate the Gaussian random number from the equations below

$$t = \sqrt{(-\ln(4(1 - \mathrm{RANX})\mathrm{RANX}))} \tag{A1a}$$

$$\mathrm{GAUSS}(t) = t(1.2378 + 0.0323t^2) \tag{A1b}$$

If RANX < 0.5 then

$$\mathrm{GAUSS}(t) = -\mathrm{GAUSS}(t) \tag{A1c}$$

The following procedure was used to obtain random coordinates on the surface of a sphere with a unit radius: (i) Generate two random number between 0 and 1, here called RANZ and RANV. (ii) Calculate the coordinates from the equations below:

$$\mathrm{RANSX} = \sqrt{1 - \mathrm{RANSZ}^2}\cos(2\pi\mathrm{RANV}) \tag{A2a}$$

$$\mathrm{RANSY} = \sqrt{1 - \mathrm{RANSZ}^2}\sin(2\pi\mathrm{RANV}) \tag{A2b}$$

where

$$\mathrm{RANSZ} = \sin(1 - 2\mathrm{RANZ})(1 - 2\sqrt{\mathrm{RANZ}(1 - \mathrm{RANZ})}) \tag{A2c}$$

Appendix B

At steady state, the concentration profile, $C(x,y,z)$, of monomers in the continuous solvent is obtained from the Laplace equation

$$\frac{\partial^2 C}{\partial x^2} + \frac{\partial^2 C}{\partial y^2} + \frac{\partial^2 C}{\partial z^2} = 0 \tag{B1}$$

with the boundary conditions

$$C = C_1 \text{ at the surface of droplet 1} \tag{B2a}$$

$$C = C_2 \text{ at the surface of droplet 2} \tag{B2b}$$

$$C = C_0 \text{ at infinity} \tag{B2c}$$

To solve eq B1, with the boundary conditions specified in eq B2, is rather difficult, but the problem can be simplified by introducing a bispherical coordinate system[33]

$$x = a\frac{\sin\xi}{\cosh\eta - \cos\xi}\cos\varphi \tag{B3a}$$

$$y = a\frac{\sin\xi}{\cosh\eta - \cos\xi}\sin\varphi \tag{B3b}$$

$$z = a\frac{\sinh\eta}{\cosh\eta - \cos\xi} \tag{B3c}$$

Here, the coordinate η is limited by η_1 (a negative number) at the surface of droplet 1 and by η_2 (a positive number) at the surface of droplet 2. The limits of ξ and φ are $0 < \xi < \pi$ and $0 < \varphi < 2\pi$ respectively. The parameter a is defined as

$$a = \frac{\sqrt{(L^2 - R_1^2 - R_2^2)^2 - 4\cdot R_1^2\cdot R_2^2}}{2L} \tag{B3d}$$

The eqs for the two coordinates η_1 and η_2 are

$$\sinh\eta_1 = -\frac{a}{R_1} \leftrightarrow \exp(\eta_1) = \frac{L^2 - 2aL + R_1^2 - R_2^2}{2LR_1} \tag{B4a}$$

$$\sinh\eta_2 = \frac{a}{R_2} \leftrightarrow \exp(-\eta_2) = \frac{L^2 - 2aL - R_1^2 + R_2^2}{2LR_2} \tag{B4b}$$

In the bispherical coordinate system eq B1 becomes, see ref 31

$$\frac{\partial}{\partial\eta}\left(\frac{a\sin\xi}{\cosh\eta - \cos\xi}\cdot\frac{\partial C}{\partial\eta}\right) + \frac{\partial}{\partial\xi}\left(\frac{a\sin\xi}{\cosh\eta - \cos\xi}\cdot\frac{\partial C}{\partial\xi}\right) = 0 \tag{B5}$$

The general solution to eq B5 is

$$C(\eta,\xi) = C_0 + \sqrt{\cosh\eta - \cos\xi}\cdot\sum_{l=0}^{\infty}(A_l\cdot\exp((l + 0.5)\cdot\eta) + B_l\cdot\exp(-(l + 0.5)\cdot\eta))\cdot P_l(\cos\xi) \tag{B6}$$

where P_l are Legendre polynomials of rank l and A_l and B_l constants can be determined from the boundary conditions at the surfaces of the two droplets:

$$\frac{C_1 - C_0}{\sqrt{\cosh\eta_1 - \cos\xi}} = \sum_{l=0}^{\infty}(A_l\exp((l + 0.5)\eta_1) + B_l\exp((l + 0.5)\eta_1))P_l(\cos\xi) \tag{B7a}$$

$$\frac{C_2 - C_0}{\sqrt{\cosh\eta_2 - \cos\xi}} = \sum_{l=0}^{\infty}(A_l\exp((l + 0.5)\eta_2) + B_l\exp((l + 0.5)\eta_2))P_l(\cos\xi) \tag{B7b}$$

The generating function of the Legendre polynomials, eq B8, can be used to simplify these two equations

$$\frac{1}{\sqrt{\cosh \eta_1 - x}} = \frac{\sqrt{2}\exp(0.5\eta_1)}{\sqrt{1+\exp(2\eta_1)-2x\exp(\eta_1)}} = \sqrt{2}\sum_{l=0}^{\infty}\exp((l+0.5)\eta_1)P_l(x) \quad \text{(B8a)}$$

$$\frac{1}{\sqrt{\cosh \eta_2 - x}} = \frac{\sqrt{2}\exp(-0.5\eta_2)}{\sqrt{1+\exp(-2\eta_2)-2x\exp(-\eta_2)}} = \sqrt{2}\sum_{l=0}^{\infty}\exp(-(l+0.5)\eta_2)P_l(x) \quad \text{(B8b)}$$

From eqs B7 and B8 the equations for A_l and B_l become

$$\sqrt{2}(C_1 - C_0)\exp((2l+1)\eta_1) = A_l\exp((2l+1)\eta_1) + B_l \quad \text{(B9a)}$$

$$\sqrt{2}(C_2 - C_0)\exp(-(2l+1)\eta_2) = A_l + B_l\exp(-(2l+1)\eta_2) \quad \text{(B9b)}$$

The solution of eqs B9a and B9b, is

$$A_l = \sqrt{2}\frac{(C_2 - C_0) - (C_1 - C_0)\exp((2l+1)\eta_1)}{1-\exp((2l+1)(\eta_1 - \eta_2))} \times \exp(-(2l+1)\eta_2) \quad \text{(B10a)}$$

$$B_l = \sqrt{2}\frac{(C_1 - C_0) - (C_2 - C_0)\exp(-(2l+1)\eta_2)}{1-\exp((2l+1)(\eta_1 - \eta_2))} \times \exp((2l+1)\eta_1) \quad \text{(B10b)}$$

When the hydrocarbon concentration profile in the solution surrounding the two droplets is known, the flow of hydrocarbon molecules between the two droplets during a time step Δt can be calculated. Fick's first law is used here to calculate the flow into droplet 1

$$Q_1 = \Delta t D\int_0^{\pi}\frac{2\pi a\sin\xi}{(\cosh\eta_1 - \cos\xi)}\left(\frac{\partial C}{\partial \eta}\right)_{\eta 1} d\xi = \int_{-1}^{1}\frac{\Delta t D 2\pi a}{(\cosh\eta_1 - x)}\cdot\left(\frac{\partial C}{\partial \eta}\right)_{\eta 1} dx \quad \text{(B11)}$$

The derivative $\partial C/\partial\eta$ at η_1 can be written as

$$\left(\frac{\partial C}{\partial \eta}\right)_{\eta 1} = \frac{(C_1 - C_0)\sinh\eta_1}{2(\cosh\eta_1 - x)} + \sqrt{\cosh\eta_1 - x}\sum_{l=0}^{\infty}(A_l\exp((l+0.5)\eta_1) - B_l\exp(-(l+0.5)\eta_1))(l+0.5)P_l(x) \quad \text{(B12)}$$

This means that the flow of hydrocarbon molecules into droplet 1 can be written as

$$\frac{Q_1}{\Delta t D} = \pi a(C_1 - C_0)\int_{-1}^{1}\frac{\sinh\eta_1}{(\cosh\eta_1 - x)^2}dx + \sum_{l=0}^{\infty}(A_l\exp((l+0.5)\eta_1) - B_l\exp(-(l+0.5)\eta_1))\int_{-1}^{1}\frac{2\pi a^2(l+0.5)}{\sqrt{(\cosh\eta_1 - x)}}P_l(x)\,dx \quad \text{(B13)}$$

The first of the two integrals in eq B13 is easy to solve

$$\int_{-1}^{1}\frac{\sinh\eta_1}{(\cosh\eta_1 - x)^2}dx = \frac{2}{\sinh\eta_1} \quad \text{(B14)}$$

The second is more complicated but can be simplified by use of the generating function of the Legendre polynomials

$$\frac{P_l(x)}{\sqrt{(\cosh\eta_1 - x)}} = \frac{\sqrt{2}\exp(0.5\eta_1)P_l(x)}{\sqrt{(1+\exp(2\eta_1) - x\exp(\eta_1))}} = \sqrt{2}\sum_{m=0}^{\infty}\exp((m+0.5)\eta_1)P_m(x)\,P_l(x) \quad \text{(B15)}$$

If eq B15 is used in the last integral of eq B13 the integration is a standard procedure. A further simplification, due to the orthogonality of the Legendre polynomials, is that all terms where $m \neq l$ becomes zero in the integration and the solution to the integral becomes

$$\int_{-1}^{1}\frac{\Delta t\cdot D\cdot 2\pi\cdot a\cdot(l+0.5)}{\sqrt{(\cosh\eta_1 - x)}}\cdot P_l(x)dx = \Delta t\cdot D\cdot\sqrt{2}\cdot 2\pi\cdot a\cdot\exp((l+0.5)\cdot\eta_1) \quad \text{(B16)}$$

If eqs B14 and B16 are used in eq B13, the equation for the flow Q_1 becomes

$$Q_1 = \Delta t D 2\pi a\left((C_1 - C_0)\cdot\frac{1}{\sinh\eta_1} + \sum_{l=0}^{\infty}(A_l\exp((2l+1)\eta_1) - B_l)\sqrt{2}\right) \quad \text{(B17)}$$

Equation B17 can be further simplified if the connection between A_l and B_l in eq B9a together with eq B4a is used

$$Q_1 = \Delta t D 4\pi R_1\left(-(C_1 - C_0) + \sqrt{2}\frac{a}{b_1}\sum_{l=0}^{\infty}A_l\exp((2l+1)\eta_1)\right) \quad \text{(B18)}$$

Further, if the equation for A_l (eq B10a) is used in eq B18, the oil flow into droplet 1 can be written as

$$Q_1 = \Delta t D 4\pi R_1((C_0 - C_1) + (C_0 - C_1)G(\eta_1,\eta_2) + (C_2 - C_0)F(\eta_1,\eta_2)) \quad \text{(B19)}$$

where

$$F(\eta_1,\eta_2) = 2\frac{a}{R_1}\sum_{l=0}^{\infty}\frac{\exp((2l+1)(\eta_1 - \eta_2))}{1-\exp((2l+1)(\eta_1 - \eta_2))} \quad \text{(B20a)}$$

and

$$G(\eta_1,\eta_2) = 2\frac{a}{R_1}\sum_{l=0}^{\infty}\frac{\exp((2l+1)(2\eta_1-\eta_2))}{1-\exp((2l+1)(\eta_1-\eta_2))} \quad \text{(B20b)}$$

Equation B19 together with eqs B20a and B20b can be used in analytical calculations but are to complicated to be used in a simulation. Therefore, we are simplifying these equations by introducing suitable approximations.

To simplify the calculations, two parameters X_1 and X_2 are introduced

$$X_1 = (L^2-(R_1+R_2)^2)/(R_1R_2) \quad \text{(B21a)}$$

$$X_2 = R_2/R_1 \quad \text{(B21b)}$$

With these new parameters, the equation for $\exp(\eta_1-\eta_2)$ becomes

$$\exp(\eta_1-\eta_2) = \left(-\frac{a}{R_1}+\sqrt{\left(\frac{a}{R_1}\right)^2+1}\right)\times \left(-\frac{a}{R_2}+\sqrt{\left(\frac{a}{R_2}\right)^2+1}\right) = \frac{1}{4L^2R_1R_2}((L^2-2aL)^2-(R_1^2-R_2^2)^2) = \frac{1}{2R_1R_2}\cdot(L^2-2aL-R_1^2-R_2^2) = 1+0.5X_1-\sqrt{X_1+0.25X_1^2} \quad \text{(B22)}$$

The parameter a can also partly be written as a function of X_1:

$$a = \frac{\sqrt{(L^2-R_1^2-R_2^2)^2-4\cdot R_1^2R_2^2}}{2L} = \frac{R_1R_2}{L}\sqrt{X_1+0.25X_1^2} \quad \text{(B23)}$$

This means that $F(\eta_1, \eta_2)$ can be written as

$$F(\eta_1,\eta_2) = 2\frac{R_2}{L}F_0(X_1) \quad \text{(B24a)}$$

where

$$F_0(X_1) = \sqrt{X_1+0.25X_1^2}\cdot \sum_{l=0}^{\infty}\frac{(1+0.5X_1-\sqrt{X_1+0.25X_1^2})^{2l+1}}{1-(1+0.5X_1-\sqrt{X_1+0.25X_1^2})^{2l+1}} \quad \text{(B24b)}$$

We have plotted $F_0(X_1)$ as a function of X_1, in the range $0.001 < X_1 < 1000$, and with a curve fit, the function line could be described with eq B25

$$F_0(X_1) \approx 0.5 + 0.25\ln\left(1+\frac{1.770}{X_1}\right) \quad \text{(B25)}$$

This means that the function $F(\eta_1, \eta_2)$, as an approximation, can be written as

$$F(\eta_1,\eta_2) \approx \frac{R_2}{L}\left(1+0.5\ln\left(1+\frac{1.770R_1R_2}{(L^2-(R_1+R_2)^2)}\right)\right) \quad \text{(B26)}$$

The $G(\eta_1, \eta_2)$ function is more complicated to approximate, because it depends both on X_1 and X_2. The function $G(\eta_1, \eta_2)$ was plotted as a function of X_1, in the range $0.0001 < X_1 < 1000$, for five different values of X_2.

Curve fits to the function lines yielded the function below:

$$G(X_1,X_2) \approx \frac{0.5}{1+1/X_2}\ln\left(1+\frac{2(1+1/X_2)}{X_1}\right) \quad \text{(B27)}$$

This means that the function $G(\eta_1, \eta_2)$, as an approximation, can be rewritten as

$$G(\eta_1,\eta_2) \approx 0.5\frac{R_2}{R_1+R_2}\ln\left(1+\frac{2R_1(R_1+R_2)}{(L^2-(R_1+R_2)^2)}\right) \quad \text{(B28)}$$

Inserting eqs B26 and B28 into eq B19 gives an expression for the calculation of oil flow between two droplets.

References and Notes

(1) *Modern Aspects of Emulsion Science*; Binks, B. P., Ed.; The Royal Society of Chemistry: Cambridge, 1998.
(2) *Encyclopedia of Emulsion Technology*; Becher, P., Ed.; Marcel Dekker: New York, 1983; Vol. 1.
(3) Evans, D. F.; Wennerström, H. *The Colloidal Domain. Where Physics, Chemistry, and Biology Meet.*, 2nd ed; Wiley-VCH: New York, 1999.
(4) Olsson, U.; Wennerström, H. *Adv. Colloid Interface Sci.* **1993**, *49*, 113.
(5) Wennerström, H.; Morris, J.; Olsson, U. *Langmuir* **1997**, *13*, 6972.
(6) Yarranton, H. W.; Masliyah, J. H. *J. Colloid. Interface. Sci.* **1997**, *196*, 157.
(7) Tikare, V.; Cawley, J. D. *Acta Mater.* **1998**, *46*, 1333.
(8) Tikare, V.; Cawley, J. D. *Acta Mater.* **1998**, *46*, 1343.
(9) Voorhees, P. W.; Glicksman, M. E. *Acta Metall.* **1984**, *32*, 2001.
(10) Voorhees, P. W.; Glicksman, M. E. *Acta Metall.* **1984**, *32*, 2013.
(11) Yao, H. J.; Elder, K. R.; Guo, H.; Grant, M. *Phys. Rev. B* **1993**, *47*, 14110.
(12) Sagui, C.; Desai, R. C. *Phys. Rev. E* **1995**, *52*, 2822.
(13) De Smet, Y.; Deriemaeker, L.; Finsy, R. *Langmuir* **1997**, *13*, 6884.
(14) Raic, K. T. *Surf. Coat. Technol.* **1997**, *92*, 22.
(15) Akaiwa, N.; Meiron, D. I. *Phys. Rev. E* **1995**, *51*, 5408.
(16) Lifshitz, I. M.; Slyozov, V. V. *J. Phys. Chem. Solids* **1961**, *19*, 35.
(17) Wagner, C. *Z. Elektrochem.* **1961**, *65*, 581.
(18) Olsson, U.; Schurtenberger, P. *Langmuir* **1993**, *9*, 3389.
(19) Olsson, U.; Bagger-Jörgensen, H.; Leaver, M.; Morris, J.; Mortensen, K.; Strey, R.; Schurtenberger, P.; Wennerström, H. *Progr. Colloid Sci.* **1997**, *106*, 6.
(20) Bagger-Jörgensen, H.; Olsson, U.; Mortensen, K. *Langmuir* **1997**, *13*, 1413.
(21) Leaver, M. S.; Olsson, U.; Wennerström, H.; Strey, R. *J. Phys. II* **1994**, *4*, 515.
(22) Evilevitch, A.; Jönsson, B.; Olsson, U.; Wennerström, H. *Langmuir* **2001**, *17*, 6893.
(23) Evilevitch, A.; Olsson, U.; Jönsson, B.; Wennerström, H. *Langmuir* **2000**, *16*, 8755.
(24) Egelhaaf, S.; Olsson, U.; Schurtenberger, P.; Morris, J.; Wennerström, H. *Phys. Rev. E* **1999**, *60*, 5681.
(25) Morris, J.; Olsson, U.; Wennerström, H. *Langmuir* **1997**, *13*, 606.
(26) Jóhannsson, R.; Almgren, M. *Langmuir* **1993**, *9*, 2879
(27) Mays, H.; Pochert, J.; Ilgenfritz, G. *Langmuir* **1995**, *11*, 4347
(28) Taisne, L.; Walstra, P.; Cabane, B. *J. Colloid Interface Sci.* **1996**, *184*, 378.
(29) Leaver, M. L.; Olsson, U.; Wennerström, H.; Strey, R.; Würz, U. *J. Chem. Soc., Faraday Trans.* **1995**, *91*, 4269.
(30) Hayduk, W.; Laudie, H. *AIChE J.* **1974**, *20*, 611.
(31) McAuliffe, C. *J. Phys. Chem.* **1966**, *70*, 1267.
(32) Le, T. D.; Olsson, U.; Wennerström, H.; Schurtenberger, P. *Phys. Rev. E* **1999**, *60*, 4300.
(33) Arfken, G. B.; Weber, H. *Mathematical Methods for Physicists*, 4th ed; Academic Press Limited: London, 1995.